1. Amenah E. kanaan [1], 2. Saba F. Ahmed Jaf [2]

University of Ninevah (1), *University of kirkuik* (2)
ORCID: 1. 0000-0001-5628-3642; 2. 0000-0001-5937-2034

doi:10.15199/48.2023.04.16

Design linear array antenna for cellular system

Abstract. *In this study, a linear array of antenna arrays, including beam scanning, lateral global connections, element designs, and bars, was developed using an antenna toolbox, guidance, and analysis on a 9-cell linear array of half-way wavelength dipoles. It aims to display a linear array model at the angle and central element patterns at the design frequency for 3D and 2D elements. For this study, the resonant dipole will be allocated to a single linear array radiator by selecting a frequency of 1,8 GHz for the design. Disposition at the resonance frequency of isolated dipole tuning. To provide the other parts with a reference impedance for the patterns, every component spirals independently. The effect of the phenomenon should not be determined by the excitement of others but should also be supported by the development of currents for each item in the array. The standardized central element pattern was monitored using standardized 9-dipole linear width management.*

Streszczenie*. W tym badaniu opracowano liniowy układ układów anten, w tym skanowanie wiązki, boczne połączenia globalne, projekty elementów i pręty, przy użyciu zestawu narzędzi antenowych, wskazówek i analizy na 9-komorowym układzie liniowym dipoli o połowie długości fali. Ma na celu wyświetlenie liniowego modelu szyku pod kątem i wzorców elementów centralnych z częstotliwością projektową dla elementów 3D i 2D. W tym badaniu dipol rezonansowy zostanie przydzielony do pojedynczego promiennika liniowego, wybierając częstotliwość 1,8 GHz do projektu. Dyspozycja przy częstotliwości rezonansowej izolowanego strojenia dipolowego. Aby zapewnić pozostałym częściom impedancję odniesienia dla wzorów, każdy element kręci się spiralnie niezależnie. Efekt zjawiska nie powinien być determinowany przez podniecenie innych, ale powinien być również wspierany przez rozwój prądów dla każdego elementu w szyku. Standaryzowany wzór elementu centralnego monitorowano przy użyciu znormalizowanego 9-dipolowego zarządzania szerokością liniową*. (**Projekt anteny liniowejdla systemu komórkowego**)

Keywords: Linear array antenna, Directivity, Azimuth, Array factor, Broadside.
Słowa kluczowe: antena liniowa, system komórkowy

Introduction

Particularly, the massive advancement in the 1950s and 1960s made the antenna range an essential technology for numerous applications, including radar, communications, remote sensing, navigation, biomedical imaging, automotive, and many more[1]–[3].Continuous development in the field of wireless applications and services has helped design current antenna[4]–[7]. By properly energizing each element to maximize

the signal over specific distances from the desired customer, arrays could also produce the desired radiation properties[8]–[10]. In one azimuth direction, the linear array performs well and has the narrowest central lobe; however, in all other azimuth directions, it performs poorly. Additionally, a significant flaw in the array is that it has a very large lobe with the same strength on the opposite side[11], [12] .The symmetry of a circular structure delivers an recognizable advantage, since it does not consist of edge components. The array plane can turn the directional designs synthesized like the circular array electronically without significant beam shape change[13]–[15]. Phase ambiguity exists in the linear arrays, and estimates' precision is constrained in the end-fire direction, particularly for those arrays with fewer terminal components. Antennas combined also reduce the accuracy of the test, which is usually compensated for by reciprocal matrix connection[16], [17]. The design and simulation of the 2.4GHz rectangular panel patch antenna showed a wireless radiation pattern at a broad beam angle and achieving a gain of 11.6dBi in 2012[18], [19]. The rectangular microstrip patch antenna was analyzed and the different substrates were compared with Ansof/Ansys HFSS and different results were shown on the same parameter[20], [21] . During 2019, two general antenna selection techniques appeared in the selection of the focused antenna subsets[21], [22]. Subsequently, for the low-intensity period of arrival, an approximation of the first arrival route (FAP) that contains the current AoA information is obtained. Finally, with one of the traditional subspace methods, the FAP signal is processed to estimate the AoA efficiently[23]. They also suggest a mixed analog, digital estimation structure based on an application of the technique for the simplification of the system architecture by means of sum difference signal patterns with slight performance loss[23]. The proposed method can provide accurate AoA predictions and significantly reduce the overall system complexity compared to the lens-less MAA system, as shown by the simulated root mean error rate curves based on the signal-to-noise ratio[24] . The use of MATLAB simulations was proposed in 2020 as a primary stage in recognizing suitable antennas for special UHF communication connectors. These fractal antennas have interesting features. Then, in a combination of urban and flat-scale circumstances, attempted to assess several of their important parameter to the one of the monopoly antenna to confirm signal protection among two real locations 5.62km away. They started with the requirements for the antenna return and link border, then they recognized their wanted thresholds, and finally, they came up with keys regarding the type of antenna in the set that delivers the peak received capacity as well as the frequency of its sub bands [25].

the subsequent sections of the article explain the Modeling and design of the suggested antenna, results obtained after computing the design and the conclusion of this work respectively‹By studying the theory analysis for the linear array equation type ‹while In a simulation results, In the antenna toolbox, we investigate the design and analysis of antenna arrays, concentrating on ideas such as beam scanning.

The analysis

The single-element antennas' emission patterns are comparatively vast when it comes to time, i.e. (gain). Antennas with very high directness are frequently required in long distance communication. The extents of the radiating component (extreme dimension far greater than μ) can be constructed by this kind of antenna. However, this approach may result in several lateral lobes and technologically unpleasant forms and dimensions. Another way of increasing an antenna's electrical size is through an electrical and geometrical assembly of radiating elements - an antenna panel. The elements of the array are normally the same. This isn't necessary, but for design and

construction it is more practical, simple and convenient. Elements of any kind may be different (wire dipoles or loops, apertures, etc.) Figure 1. Display the array of two items in the far-zone of the array components, let us represent the electric fields:

$$\overrightarrow{E_1} = M_1 E_{n_1}(\theta_1, \emptyset_1) \frac{e^{-j(kr_1 - \frac{\beta}{2})}}{r_1} \widehat{p_1} \quad (1)$$

whre: M1 and M2 field magnitudes (without taking the 1/r factor into account); En1 , En2 uniform field patterns; r 1, r 2 distance to observation point P ; β phase difference between the feeds of the two array elements; ρ ˆ1 , ρ ˆ2 polarization vectors of the far-zone E fields.

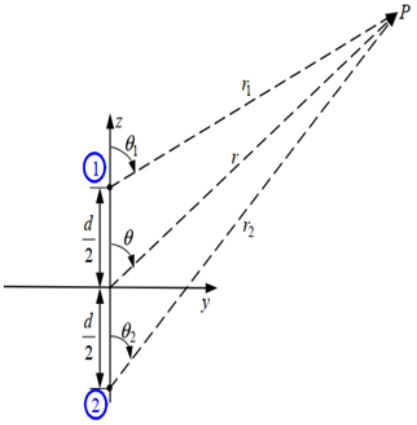

Fig.1. 2 - an array of linear components with constant amplitude and spacing.

$$\overrightarrow{E_2} = M_2 E_{n_2}(\theta_2, \emptyset_2) \frac{e^{-j(kr_2 + \frac{\beta}{2})}}{r_2} \widehat{p_2} \quad (2)$$

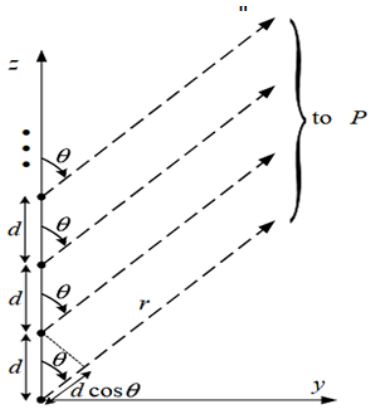

Fig.2. uniform amplitude and spacing N-element linear array.

Every succeeding component is thought to have β enhanced current excitement over the preceding component. A progressive phase and an array of identical elements are characteristics of a uniform array. The AF can be obtained from the point (isotropic) sources of the individual elements. Where the items have a different pattern, it is possible to achieve the total pattern by just multiplying the AF by the normalized field pattern of a single element. The array factor (AF) from an N-element linear array of isotropic sources with constant amplitude and spacin

$$AF = 1 + e^{j(kd\cos\theta+\beta)} + e^{j2(kd\cos\theta+\beta)} + \ldots + e^{j(N-1)(kd\cos\theta+\beta)} \quad (3)$$

Where figure 3. Shows the geometrical construction for the array factor , Phase terms in partial field:

$$1^{st} \rightarrow e^{-jkr}$$
$$2^{nd} \rightarrow e^{-jk(r-d\cos\theta)}$$
$$3^{rd} \rightarrow e^{-jk(r-2d\cos\theta)}$$
$$\ldots$$
$$N^{th} \rightarrow e^{-jk(r-(N-1)d\cos\theta)} \quad (4)$$

Equation (3) can be re- written as :

$$AF = \sum_{n=1}^{N} e^{j(n-1)(kd\cos\theta+\beta)} \quad (5)$$

Equation (5) shows how AFs can be controlled by a comparative phase (β) between elements. The overall antenna pattern can be adjusted using five simple techniques: The entire range is first set up geometrically, using shapes like linear, circular, spherical, rectangular, etc. The second method is the relative displacement of elements, and the third method is the excitement of each element, with the fourth method being the excitation phase, and the last method being the relative pattern of each element.

Simulation results

A perception, such as beam scanning in a simulation, is the focus of analysis and generation of arrays in the antenna toolbox. Tests were performed on a linear array of nine elements. For the design frequency, choose 1.8 GHz. The figure. 4(a) by defining array-size, N and element-to-element spacing, dx. The dipole, where the first length is chosen is the separate element of the array. A single radiator with a linear range is the resonant dipole. Once the isolated dipole was tuned to the resonance at the design frequency, the area around the array was cleaned.

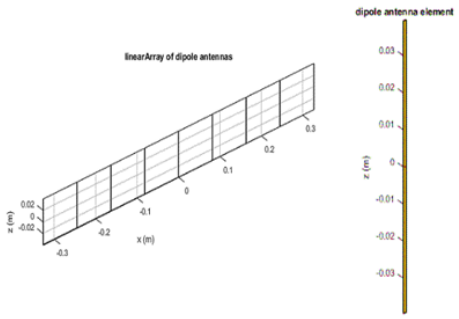

Fig..4 (a) linear array of half-wavelength dipoles (b) Observe the array's geometry and the component number and spacing.

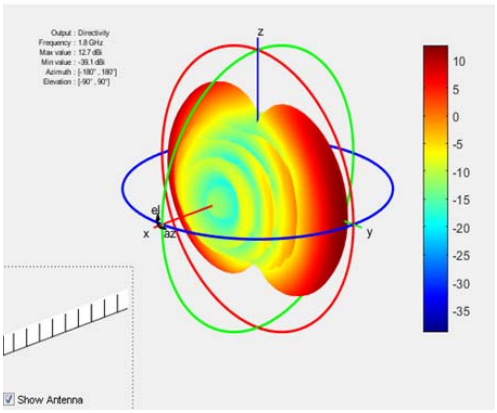

Fig. 5. The 3D spatial representation of the linear array's design frequency pattern.

The azimuthal angle of the array is 90 deg, showing the beam maximum. Plot the azimuthal (x-y) plane 2D radiation pattern corresponding to the nil lifting angle. Where Figure 6 displays the 3D design frequency linear array pattern. Figure 6 displays The following, in (a) (a) The array has a maximum directive of 12.83 dBi, and the first side lobes are about 13 dB down on either side of the peak. This is due to the uniform amplitude taper of the array feeding all elements in 1V.

a)

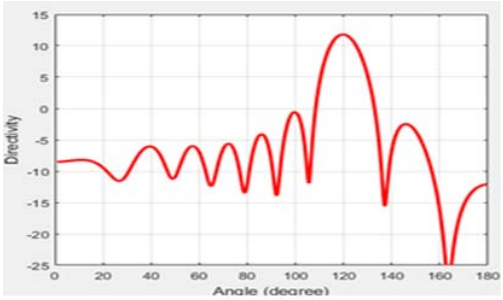

b)

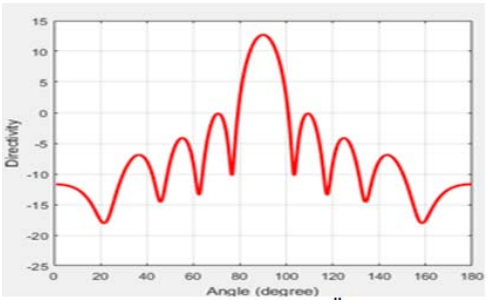

Fig. 6. (a) the azimuthal plane (x-y plane) 2D radiation pattern plot. (b) In the azimuthal plane (x-y plane), plot the 2D radiation pattern scanning.

Note a decrease in direction of approximately 0.9 dB. This drop increases for infinite arrays, given the growing scan angle in line with the cosine law. Every element's pattern can vary considerably in small arrays. We intend to design the central components and two-edge electors in order to verify this fact. Using a reference impedance to the patterns, stir each component separately before completing the mixture. From left to right along the x axis, the elements are numbered.

The arrangement of the elements demonstrates that every other image is reflected in the plot's center, with the first element's pattern acting as a reflective mirror of the ninth element's azimuth of 90 degrees, as shown in Figure 7.

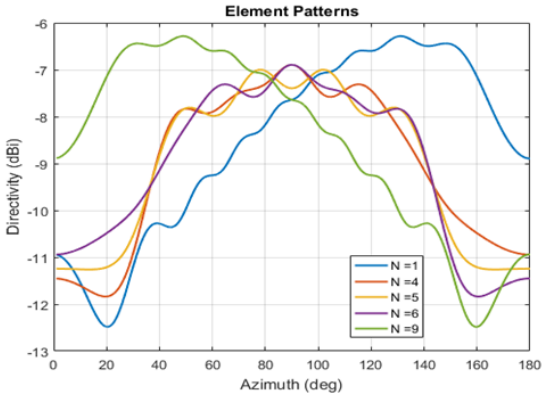

Fig.7. The plot of the element patterns.

Conclusion

This paper examines a linear array of half-wave dipole systems, such as the beam scanning process. A linear array of 9 elements with a toolbox antenna is scanned and analyzed. Likewise, Frequency of 1,8 GHz and attachment of each linear beam at the resonant dipole were studied, is isolated dipole was tuned to the resonance of the frequency of design, the linear 3D and 2D corner patterns of the panels and the central design frequency item patterns drafted as shown in Figure 5.6 by using the toolbox antenna program. In small arrays, the pattern of each element was significantly different from the other patterns, according to the results. This was confirmed when the design has been implemented with the main elements and two edge electors. The array had a maximum directive of 12.83 dBi according to the results of the toolbox program and the first sidelobes were approximately 13 dB down on either side of the upper end. The uniform amplitude taper of the array feeding all elements in 1V is responsible.

Authors: Amenah E. Kanaan Mrs. Amenah holds a Bachelor's degree in Electrical/Electronic and Communications Engineering from Mosul University. She can be contacted at amenah.kanaan@uoninevah.edu.iq. Saba F. Ahmed Jaf holds a Bachelor's degree in Electrical/Electronic and Communications Engineering from kirkuik University. She can be contacted Saba.eng81@kirkuk.edu.iq.

REFERENCES

[1] C. A. Fowler, “Old radar types never die; they just phased array or... 55 years of trying to avoid mechanical scan,” *IEEE Aerosp. Electron. Syst. Mag.*, vol. 13, no. 9, pp. 24A-24L, 1998.

[2] D. K. Cheng, “Optimization techniques for antenna arrays,” *Proc. IEEE*, vol. 59, no. 12, pp. 1664–1674, 1971.

[3] R. C. Hansen, “Fundamental limitations in antennas,” *Proc. IEEE*, vol. 69, no. 2, pp. 170–182, 1981.

[4] Y.-L. Ban, Y.-F. Qiang, Z. Chen, K. Kang, and J.-H. Guo, “A dual-loop antenna design for hepta-band WWAN/LTE metal-rimmed smartphone applications,” *IEEE Trans. Antennas Propag.*, vol. 63, no. 1, pp. 48–58, 2014.

[5] J. Anguera, A. Andújar, M.-C. Huynh, C. Orlenius, C. Picher, and C. Puente, “Advances in antenna technology for wireless handheld devices,” *Int. J. Antennas Propag.*, vol. 2013, 2013.

[6] T. Ali, A. W. M. Saadh, R. C. Biradar, J. Anguera, and A. Andújar, “A miniaturized metamaterial slot antenna for wireless applications,” *AEU-International J. Electron. Commun.*, vol. 82, pp. 368–382, 2017.

[7] S. Ghosh and D. Sen, “An inclusive survey on array antenna design for millimeter-wave communications,” *IEEE Access*, vol. 7, pp. 83137–83161, 2019.

[8] A. A. Qasim and A. H. Sallomi, “Design and Analysis of Phased Array System by MATLAB Toolbox,” *Al-Kitab J. Pure Sci.*, vol. 4, no. 1, 2020.

[9] R. C. Baumann, “Radiation-induced soft errors in advanced semiconductor technologies,” *IEEE Trans. Device Mater. Reliab.*, vol. 5, no. 3, pp. 305–316, 2005.

[10] M. A. S. Natera *et al.*, “New antenna array architectures for satellite communications,” in *Advances in Satellite Communications*, IntechOpen, 2011.

[11] T.-Y. Kim and S.-S. Hwang, “Performance Analysis of Beamforming Satellite System Applying Circular Array Antenna,” *J. Korea Inst. Electron. Commun. Sci.*, vol. 14, no. 5, pp. 845–852, 2019.

[12] A. Vesa, F. Alexa, and H. Baltă, “Comparisons between 2D and 3D uniform array antennas,” in *2015 Federated Conference on Computer Science and Information Systems (FedCSIS)*, 2015, pp. 1285–1290.

[13] O. Quevedo-Teruel *et al.*, “Roadmap on metasurfaces,” *J. Opt.*, vol. 21, no. 7, p. 73002, 2019.

[14] O. Tsilipakos *et al.*, “Toward intelligent metasurfaces: the progress from globally tunable metasurfaces to software-defined metasurfaces with an embedded network of controllers,” *Adv. Opt. Mater.*, vol. 8, no. 17, p. 2000783, 2020.

[15] P. Ioannides and C. A. Balanis, “Uniform circular arrays for smart antennas,” *IEEE Antennas Propag. Mag.*, vol. 47, no. 4, pp. 192–206, 2005.
[16] B. Liao, Z.-G. Zhang, and S.-C. Chan, “DOA estimation and tracking of ULAs with mutual coupling,” *IEEE Trans. Aerosp. Electron. Syst.*, vol. 48, no. 1, pp. 891–905, 2012.
[17] L. D. Girod, *A self-calibrating system of distributed acoustic arrays*. University of California, Los Angeles, 2005.
[18] A. Pal, A. Mehta, D. Mirshekar-Syahkal, and H. Nakano, “$2\times2 $ Phased Array Consisting of Square Loop Antennas for High Gain Wide Angle Scanning with Low Grating Lobes,” *IEEE Trans. Antennas Propag.*, vol. 65, no. 2, pp. 576–583, 2016.
[19] Y. F. Cao and X. Y. Zhang, “A wideband beam-steerable slot antenna using artificial magnetic conductors with simple structure,” *IEEE Trans. Antennas Propag.*, vol. 66, no. 4, pp. 1685–1694, 2018.
[20] V. Mathur and M. Gupta, “Comparison of performance characteristics of rectangular, square and hexagonal microstrip patch antennas,” in *Proceedings of 3rd International Conference on Reliability, Infocom Technologies and Optimization*, 2014, pp. 1–6.
[21] R. Najeeb, D. Hassan, D. Najeeb, and H. Ademgil, “Design and simulation of microstrip patch antenna array for X-Band applications,” in *2016 HONET-ICT*, 2016, pp. 79–83.
[22] N. P. Le and F. Safaei, “Antenna selection strategies for MIMO-OFDM wireless systems: An energy efficiency perspective,” *IEEE Trans. Veh. Technol.*, vol. 65, no. 4, pp. 2048–2062, 2015.
[23] L. Li *et al.*, “mmWave communications for 5G: implementation challenges and advances,” *Sci. China Inf. Sci.*, vol. 61, no. 2, p. 21301, 2018.
[24] S. A. Shaikh and A. M. Tonello, “Radio source localization in multipath channels using EM lens assisted massive antennas arrays,” *IEEE Access*, vol. 7, pp. 9001–9012, 2019.
[25] D. Vatamanu and S. Miclăuş, “UHF Fractal Antennas: Solutions for Radio Links Using Matlab Simulations,” in *International Conference Knowledge-Based Organization*, 2020, vol. 26, no. 3, pp. 179–184.